Flight Control of the Model 192

1.0 The basic flight control modes of the Model 192 may be summarized as follows:

1.1 Primary mode - three axis control augmentation

1.2 Automatic mode - three axis autopilot

1.3 Emergency mode - three axis direct manual control

1.4 Manual thrust control during boost

1.5 Manual speed brake control during landing

The pilot's compartment is equipped with an efficient set of controls to provide the pilot with optimum utilization of the above available modes plus complete position, navigation, energy management and safety boundary instrumentation to help him fly the mission, select the best landing site, and use abort procedures if required.

A two axis side arm controller is provided on the right hand console to accomplish pitch and roll control of the primary mode. Rudder deflection required for yaw damping and turn coordination is automatically provided in all modes except emergency manual control, for which conventional rudder pedals are provided. A pitch trim wheel is located in the top of the side stick and a disengage button is provided for disengaging the automatic modes. The side stick pitch pivot is located approximately at the center of pressure of the pilots hand and the roll pivot is along the axis of his forearm to minimize control problems during acceleration of the vehicle. A control panel is located on the left hand console to provide selection of the various modes of automatic control, trim switches for roll and yaw during modes 1.1 and 1.2, and a manual gain adjustment. Also located on this panel are three levers used for mechanically

1.0 (Continued)

disengaging the three individual axes of control augmentation. Operation of one of these levers places control of the corresponding axis under the emergency manual mode which utilizes a conventional center stick and rudder pedals which are connected to their associated control surfaces through mechanical linkage and dual hydraulic actuators. Levers for throttle and speed brake control are located on the left hand console. The throttle lever is pivoted similar to the pitch axis of the side stick controller to minimize acceleration effects on manual throttle manipulation. Throttle detents are provided at the 10 and 100 percent thrust settings.

2.0 Description of Control Modes:

2.1 The primary mode of flight path control, control augmentation, is essentially a pitch and roll "fly-by-wire" mode coupled with three axis stability augmentation and turn coordination. All sensors, electrical, electronic and electro-hydraulic elements of this system are triple redundant with interstage "majority rule" voting. Each control axis can tolerate failure of a number of its system elements, including loss of one electrical and one hydraulic system, without degraded performance as long as two functionally identical components do not fail; i.e., two rate gyros, two servo amplifiers, etc. Total failure of one axis of this control mode does not deprive the pilot of full use of the remaining axes. A failed axis of the control augmentation mode may be disengaged with the L.H. console disengage lever and its function assumed by the appropriate emergency direct manual control. It should be noted that vehicles such as Gemini and

2.1 (Continued)

the X-20 (Dyna Soar) depend upon similar fly-by-wire/control augmentation schemes without the benefit of a mechanical/hydraulic manual control system for back-up in the event of failure. This "fly-by-wire" system ties into the direct manual control linkage through parallel servos so that commands generated by the side stick or by the stability augmentation system result in proportional motion of the central control stick. Motion of the rudder pedals is prevented during control augmentation by a hydraulic lock out device that is de-energized upon disengagement of the yaw axis of control augmentation thus making the pedals available to the pilot for the emergency mode.

2.2 While operating in control augmentation the pilot may select certain fully automatic control modes available in the autopilot (automatic mode). Pre-programmed boost trajectories can be supplied to the autopilot by the on-board computer. Angle of attack and bank angle hold are available during the glide with a programmed heading command input. The autopilot has the capability of coupling to a data link system to accept closed loop ground controlled automatic landing commands if operation with an automatic landing system becomes a requirement. Autopilot modes may be selected on the left hand console and disengaged there or by momentary operation of a disengage button on the side stick controller. The autopilot control console consists of the three mechanical levers for disengagement of individual control augmentation functions, trim wheels for roll and yaw, adaptive/manual gain selector and manual gain adjustment, solenoid held autopilot engage switch and solenoid

2.2 (Continued)

held selector switches for the various available autopilot mode functions.

2.3 Since it is difficult and costly (weight and dollars) to attempt to supply autopilot operation with the potential reliability inherent in the control augmentation mechanization, reliance is placed upon the pilot to navigate and fly the mission manually using control augmentation in the event of an autopilot malfunction. Momentary operation of the disengage button on the side stick reverts the vehicle from autopilot control to pilot control augmentation. In the unlikely event that an axis of control augmentation fails, representing dual failure of an individual system element, the pilot merely takes over the particular function in the manual emergency mode by pulling the appropriate control augmentation disengage lever thus disabling the parallel servo in that channel. Direct manual emergency control is provided by conventionally mechanized stick and rudder pedals. No stability augmentation is available to a control axis operated in this mode, but handling qualities without stability augmentation are predicted to be acceptable for emergency control throughout flight.

2.4 Proportional thrust control is commanded by the pilot through use of the left hand throttle lever. A detent is provided for operation of the engine at 10 percent thrust, used for prelaunch engine ignition and again just prior to cutoff as a velocity vernier and to prevent fuel pump overspeeding at cutoff. The throttle pivot is located to minimize control problems under high longitudinal acceleration. It is anticipated that the pilot will be capable of exercising precise throttle and flight path control during the acceleration environment

2.4 (Continued)

of boost based on experience with human capabilities under similar acceleration stress flying boost and re-entry of such vehicles as Mercury and Gemini and from centrifuge tests of these same missions plus Apollo re-entry. Figure 1 shows the Model 192 boost acceleration profile superimposed on these other manually controlled vehicle profiles. Centrifuge tests have confirmed the ability of astronauts to control attitude during boost using the side arm controller of Mercury, Gemini, and Apollo. Astronauts Cooper and Grissom demonstrated their capability to manually control attitude and damping during re-entry of Mercury MA-9 and Gemini GT-3 respectively. As may be seen from Figure 1 the Model 192 boost environment is less severe than that of any of the other proven control tasks.

As the Model 192 boost approaches the desired glide insertion flight conditions the pilot will monitor velocity and modulate thrust to smoothly approach the required end velocity. The last 5 to 10 seconds prior to cut off will be flown at 10 percent thrust to enable the pilot to accurately establish cut off speed.

2.5 Late in the glide the pilot concentrates on range modulation and energy management to reach the desired landing site or an available alternate site if required. Below approximately Mach 4, manually operated speedbrakes are available to assist in energy management. The pilot utilizes a control lever adjacent to his throttle lever for proportional control of speed brake deflection. Use of speedbrakes permits a range modulation capability of approximately 30 miles

2.5 (Continued)

in addition to the modulation available through angle-of-attack and bank angle control.

With the pilot in the loop during landing to take advantage of visual cues, voice communication with the ground and alternate navigation aids, the landing guidance system of the landing site can be significantly simplified over a system required to successfully land an unmanned aircraft.

Dave Thompson 20 April 65

Dave Thompson

FIGURE 1

ACCELERATION PROFILES FOR MANUALLY CONTROLLED VEHICLES

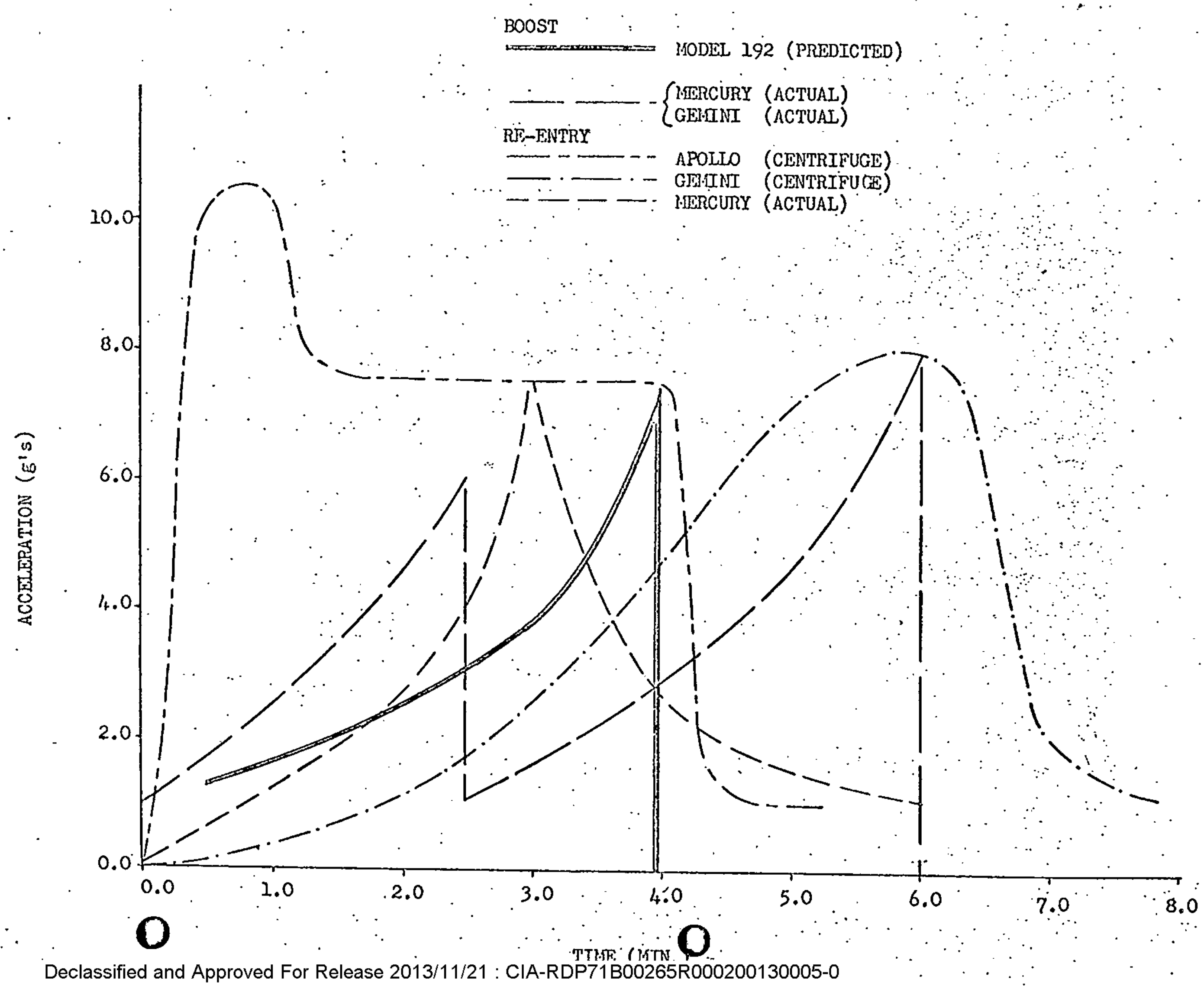

TECHNICAL DATA

$W/SC_L \sim 400$

C_L @ $(L/D)_{MAX} \sim .054$

APPROACH $L/D = 3.5$

GLIDE $L/D = 3.0$

GEAR DOWN $L/D = 2.5$

PRE-COOL TANKS WITH LOW FLOW RATE OF LO_2/LH_2

LOW VARIATION IN FLIGHT CHARACTERISTICS DON'T REQUIRE SELF ADAPTIVE CONTROL SYSTEM.

Discussions with M-H, Minn. included the following:

1. Fuel sloshing during boost - 3 rad/sec - aero surfaces are not adequate for pitch control

2. Vehicle bending frequency - 5½ cps full
8-8½ " empty
Natural frequency ~ .20 cps

3. Anticipate that most difficult control problem will occur during boost due to fuel sloshing - No baffles used because of added weight.

4. g variation during boost ~ 100-650

5. Vehicle to operate in 128 db acoustic noise while attached to B-52

6. During boost, body attitude to be held within ±.20°, flt. perturbations, i.e., gusts, to be damped to ½ amplitude in 1 sec.

7. During glide, angle of attack & sideslip to be held within ±¼°, pitch & yaw within ±.50° & roll within ±.75°

8. Assigned 50 lbs. & 895 cu. in to A/P, rate gyros, etc.

General Arrangement -

a. Gimballed engine is the primary pitch control during boost. Compensates for the fuel shift during boost. Keeps thrust going through the c.g. During boost, forces on tanks are normal & thrust. Resultant acts perpendicular to the plane of the fuel.

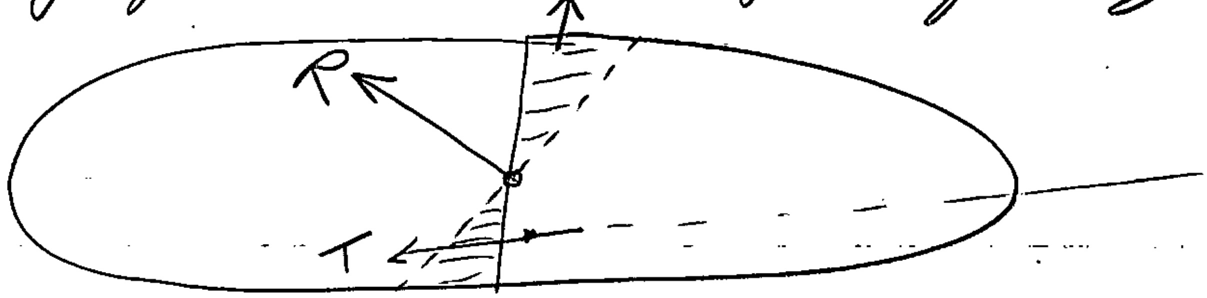

b. Boat tail gives high L/D for landing condition by reducing base drag. No effect hypersonic.

2. Composite Test Panel - For short duration, attachment area is less severe than center section because attachment bolt absorbs heat. After attachment bolt has reached equilibrium temperature, i.e., 16 min line, panel temperature increases because of heat short at attachment. Therefore increased waterwick is required.

3. Separation characteristics -
C_n variation due to the shift from the interference effects of the B-52 to free stream. The curve shows the variation in C_n if elevons are not moved. Approx $\pm 3\ 24^{\circ}$ elevon would be required to trim. Total elevon travel = 30°.

4. General arrangement:
Toe-in of verticals (6°) allows verticals to operate at max L/D. Also operates at more effective portion of curve, i.e. steeper slope so that small deflections are more significant

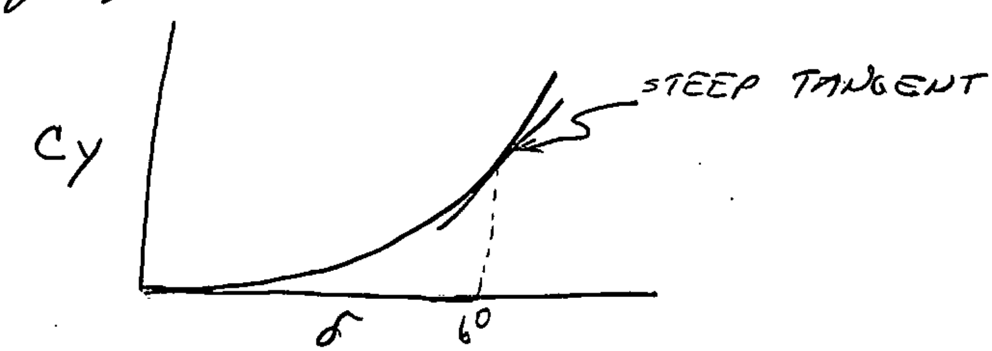

Small drag increment due to 6° offset many times by max L/D operation & smaller moveable surface required ~~#~~ due to effectiveness curve above.

5. Aerothermodynamic Vehicle Comparison.

$T \sim (V, h, \delta_B)$

$(V, h) \sim q \sim (W/S, C_L)$

$C_L \sim \delta_B$

$T \sim (W/S, \delta_B)$

Note: Temperature is equilibrium, i.e., the stabilized temperature corresponding to the vehicle being held fixed at a particular point in its trajectory until an equilibrium temperature is reached.

New curve being prepared to illustrate different trajectories due to differences in W/S & δ_B, and corresponding equilibrium temperatures.

21 JUNE 1965

Maneuvering During Hypersonic Glide

1. In hypersonic glide, maneuvering will generally be accomplished by a banked coordinated turn. Due to the high speeds involved and large distances traveled it is necessary to account for the effects of earth's curvature and rotation, otherwise classical relationships are applicable.

2. The generic hypersonic aircraft can develop lift within the restraints imposed by load factors and heating rates. If the lift is greater than that required for equilibrium glide the excess may be directed by banking for the purpose of maneuvering. The following sketch illustrates this procedure and defines certain terms.

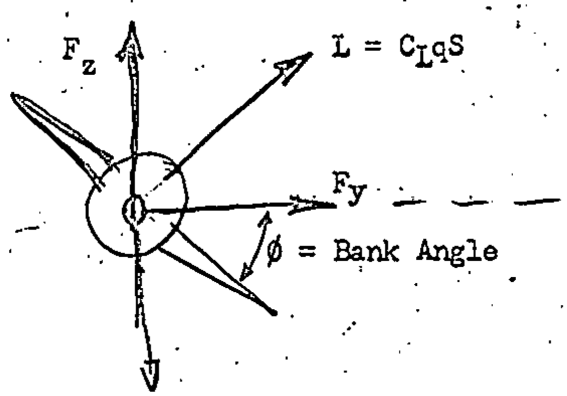

$F_z = L \cos \phi$

$F_y = L \sin \phi$

From the above sketch it is obvious that for a coordinated turn at high speeds

$$F_z = L \cos \phi = W \left(1 - \left(\frac{V_I}{V_S}\right)^2\right) \qquad (1)$$

$$F_y = L \sin \phi = \frac{m V_I^2}{r} \qquad (2)$$

where: V_I = inertial velocity

V_S = satellite velocity

r = radius of turn

By combining equations (1) and (2) the force available for maneuvering is expressed as

$$F_y = F_z \tan \phi$$

$$= W \left(1 - \left(\frac{V_I}{V_S}\right)^2\right) \tan \phi$$

$$= W \left(\frac{L}{W}\right)_{req.} \tan \phi \qquad (3)$$

where $\left(\frac{L}{W}\right)_{req.} = \left(1 - \left(\frac{V_I}{V_S}\right)^2\right)$ yields the lift component (F_Z) required for level flight in terms of the weight and is given in Fig. (1) as a function of velocity.

Since F_y is theturning force, consideration of equations (2) and (3) allows for solution of the turn radius,

$$F_y = m \frac{V_I^2}{r} = W \left(\frac{L}{W}\right)_{req.} \tan \phi$$

$$r = \frac{m V_I^2}{W \left(\frac{L}{W}\right)_{req.} \tan \phi} = \frac{V_I^2}{g \left(\frac{L}{W}\right)_{req.} \tan \phi} \qquad (4)$$

The turning rate Ω is given by

$$\Omega = \frac{V_I}{r} \qquad (5)$$

$$\Omega = \frac{(L/W)_{req.}\ g \tan \phi}{V_r} \qquad (6)$$

If the allowable load factor is specified rather than the bank angle the following relationships are useful.

$$W n_{allowable} = L \qquad (7)$$

from equation (2)

$$F_y = L \sin \phi = n W \sin \phi \qquad (8)$$

$$F_z = L \cos \phi = n W \cos \phi \qquad (9)$$

Since for equilibrium

$$F_z = W \left(1 - \left(\frac{V_I}{V_S}\right)^2 \right) = n W \cos \phi$$

$$\cos \phi = \frac{\left[1 - \left(\frac{V_I}{V_S}\right)^2\right] \cancel{W}}{n \cancel{W}}$$

$$\cos \phi_{allow} = \frac{1 - \left(\frac{V_I}{V_S}\right)^2}{n_{allow}} = \frac{(L/W)_{req}}{n_{\ allowable}}$$

$$\phi_{allow} = \cos^{-1}\left[(L/W)_{req} \cdot \frac{1}{n_{\ allow}} \right] \qquad (10)$$

where $(L/W)_{req.}$ is for wings level as given in Figure (1).

EXAMPLES

I.

V = 17,000 ft/sec

ϕ allowable = 45° (due to temperature considerations)

Solve for turn radius

From Figure (1)

(L/W) req = .568

$$r = \frac{(17,000)^2}{(32.2)(.568)(1.00)}$$

$r = 15.8 \times 10^6$ feet = 2,600 n. mi.

II.

V = 8,000 ft/sec

$n_{allowable} = 5$ (structural allowable)

Solve for turn radius

$$\phi_{allow} = \cos^{-1}\left[.905/5\right] = \cos^{-1}(.181)$$

$$= 79^\circ\ 34'$$

$\tan\phi = 5.4308$

$$r = \frac{(8,000)^2}{(32.2)(.905)(5.4308)} = 405,000 \text{ feet}$$

$r = 66.5$ n. mi.

HYPERSONIC GLIDE LIFT-TO-WEIGHT RATIO

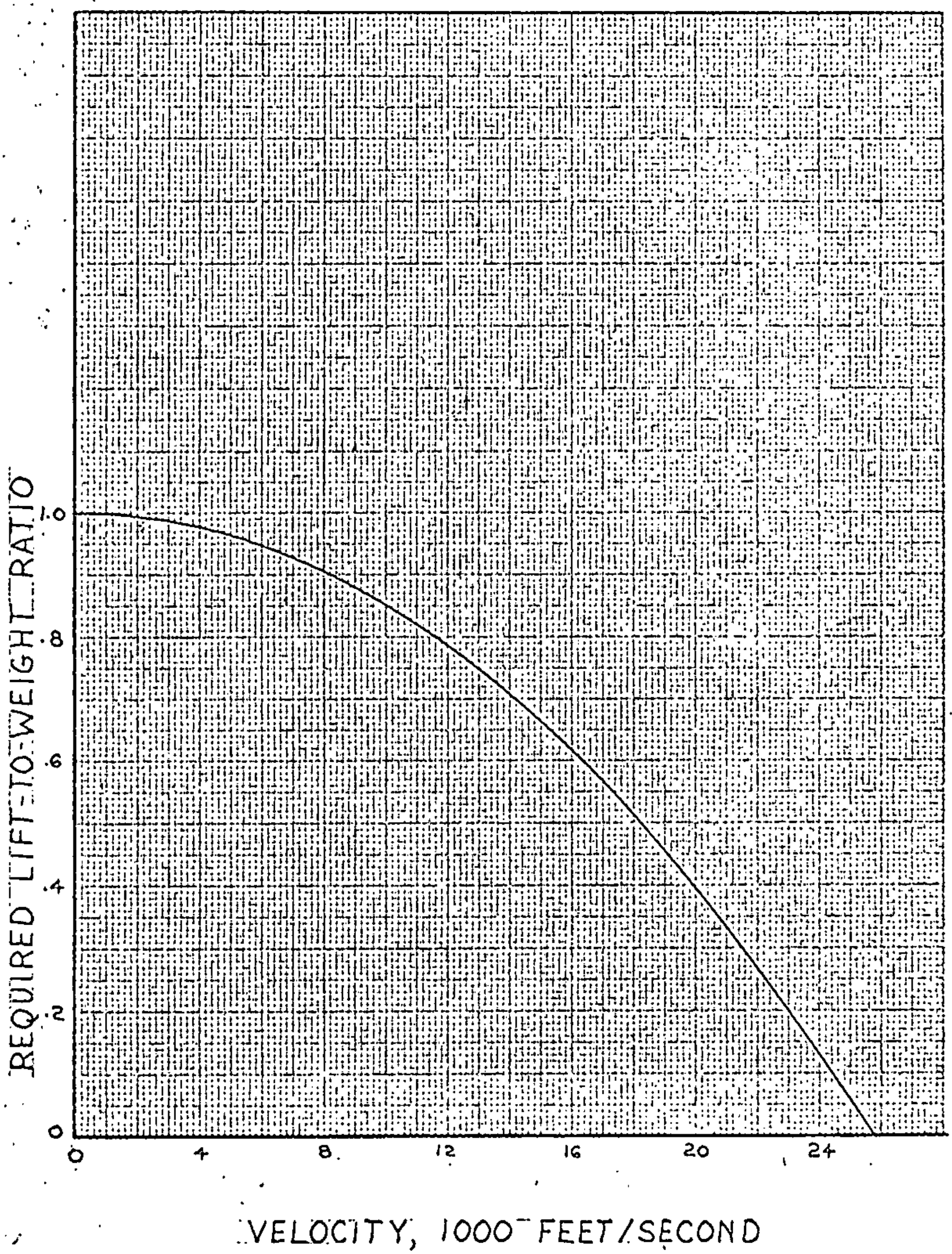

FIG. (1)

ENGINE-AIRFRAME OPTIMIZATION

Subsequent to the original optimization which arrived at the T_{VAC} = 200,000 lbs., further investigation of the energy management, i.e., the time history of the vehicle drag, has been completed. Also additional wind tunnel test results, indicating a slightly different C_{D_0} vs M variation, have become available. Using these additional and later inputs to further optimize the configuration, it appears that a T_{VAC} = 225,000 lbs. will provide an incremental range of 120 N. M. with the same fuel load. Furthermore, the thrust-to-weight ratio for the increased thrust corresponds to a more optimum point on the boost efficiency curve, i.e., velocity loss vs. T/W. A further pay-off is realized with this more optimum engine-airfram matching in that the performance sensitivity (range) to small system changes is greatly reduced.

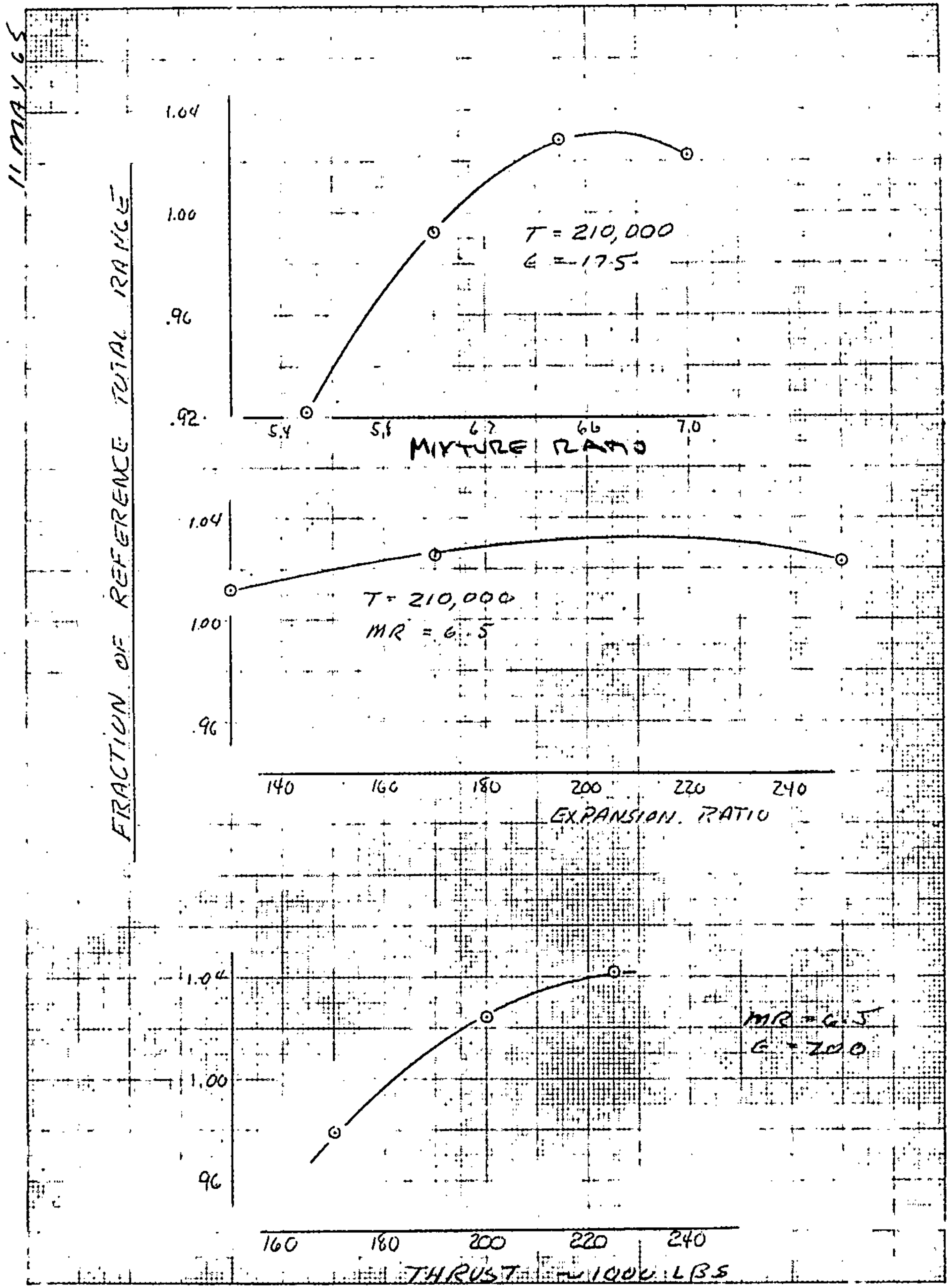
11 MAY 65
FRACTION OF REFERENCE TOTAL RANGE
1.04
1.00
.96
.92
T = 210,000
ε = 175
5.4
5.8
6.2
6.6
7.0
MIXTURE RATIO
1.04
1.00
.96
T = 210,000
MR = 6.5
140
160
180
200
220
240
EXPANSION RATIO
1.04
1.00
.96
MR = 6.5
ε = 200
160
180
200
220
240
THRUST ~ 1000 LBS

$T_{YAC} = 225,000$

(FIXED A/C STRUCTURE)

7550

	SAME ∈	SAME IMPINGEMENT	SAME RANGE
RANGE	7500	7470	7380
Δ RANGE	+120	+90	0
Δ FUEL	0	-1000	-1300
Δ WEIGHT (A/C)	0	0	0
Δ WEIGHT (ENG)	+300	+200	+300
∈	200	180	200
Δ LENGTH (ENG)	+16"	-15	+16
	(+300#)	(-800#)	(-1000#)

Δ 5% FUEL ≈ Δ 1000 LBS A/C

5360 LBS FUEL ≈ 1000 LBS A/C

Δ FUEL	0	-1000	-1300
Δ A/C STRUCT. WT	0	-186.5	-242.5
	+300#	-986.5#	-1292.5#

HYPERSONIC DRAG

The drag characteristics of blunt bodies such as Mercury and Gemini at hypersonic speeds can be predicted sufficiently well for design and reliably measured in the wind tunnel, since the major portion of the drag is pressure drag. As bodies become more slender, however, the skin friction contribution becomes of increasing importance, and accurate methods are required for skin friction estimation and for correction of model test data to full-scale conditions.

For the subsonic and low supersonic speed regimes the aerodynamicist can make good estimates of the mean skin friction coefficient of a configuration as a function of Mach number and Reynolds number by means of accepted theories or by means of test data. As velocities approach the hypersonic speed regime, effects considered negligible at lower speeds (i.e., heat transfer, temperature variation within the boundary layer, and variable fluid properties) have to be included in the friction estimates. With these additional variables in the hypersonic speed regime the simultaneous simulation of all important variables in a wind tunnel is impossible. Thus, the wind tunnel alone is no longer sufficient for determination of the frictional drag component of a vehicle. Although the exact magnitude of the friction drag of a specific configuration can not be obtained in the hypersonic wind tunnel, the aerodynamicist can still obtain wind tunnel data for which individual simulation of each of the major variables has been accomplished. Such data can then be used to substantiate or develop theories and methods which can be utilized with confidence for estimating the friction drag of flight vehicles.

At the present time most confidence is enjoyed with the use of a modification to Eckert's reference enthalpy method. This method accounts for boundary layer temperature and permits inclusion of real gas effects. The parameter by which the viscous forces on high L/D configurations may be correlated and related to free stream Mach number and Reynold's number conditions is deduced below.

The classical Blasius solution of the Navier Stokes equations for incompressible flow on a flat plate leads to the relation

$$c_f = \frac{\tau}{\frac{1}{2}\rho V^2} = \frac{0.664}{\sqrt{R_x}} = \frac{0.664}{\sqrt{\frac{\rho V x}{\mu}}} \quad . (1)$$

Eckert accounts for compressibility, local wall temperature, and real gas effects by use of a reference enthalpy. This parameter has been empirically defined as

$$h^* = .5h_{wall} + .22h_{aw} + .28h_{local} \quad (2)$$

The equation for local friction coefficient based on reference conditions then becomes

$$C_f^* = \frac{\tau_w}{\frac{1}{2}\rho^* V_L^2} = \frac{0.664}{\sqrt{R_x^*}} = 0.664\sqrt{\frac{\mu^*}{\rho^* V_L x}} \quad (3)$$

where the density and viscosity are evaluated at conditions corresponding to the reference enthalpy and the local pressure. Then, converting the local reference skin friction coefficient to the "free-stream" basis, gives

$$C_{f_\infty} = C_f^* \frac{\rho^*}{\rho_\infty}\left(\frac{V_L}{V_\infty}\right)^2 = 0.664\sqrt{\frac{\mu^*}{\rho^* V_L x}}\left(\frac{\rho^*}{\rho_\infty}\right)\left(\frac{V_L}{V_\infty}\right)^2$$

or

$$C_{f_\infty} = \frac{0.664}{\sqrt{R_{x\infty}}}\sqrt{\frac{(\mu/T)^*}{(\mu/T)_\infty}\left(\frac{P_L}{P_\infty}\right)\left(\frac{V_L}{V_\infty}\right)^3} \quad (4)$$

and C* can be substituted for

$$\frac{(\mu/T)^*}{(\mu/T)_\infty}$$

Then the total skin friction coefficient on a flat plate of length (1) is given by

$$C_{A_F} = 1.328 \sqrt{\frac{C^*}{R_{l\infty}} \left(\frac{\rho_L}{\rho_\infty}\right)\left(\frac{V_L}{V_\infty}\right)^3} \; \frac{S_{wet}}{S_{ref}} \qquad (5)$$

Conical body total skin friction coefficients may be determined by using Manglers transformation and integrating the local skin friction coefficients over the vehicle. This results in the following equations for the axial force coefficient due to skin friction on a conical body:

$$C_{A_F} = \frac{4\sqrt{3}}{3}(0.664)\sqrt{\frac{C^*}{R_{l\infty}} \left(\frac{\rho_L}{\rho_\infty}\right)\left(\frac{V_L}{V_\infty}\right)^3} \; \frac{S_{wet}}{S_{ref}} \qquad (6)$$

Thus the viscous forces for this class of body $\left(C_{A_F} \frac{S_{wet}}{S_{ref}}\right)$ are directly proportional to the parameter

$$\sqrt{\frac{C^*}{R_{l\infty}} \left(\frac{\rho_L}{\rho_\infty}\right)\left(\frac{V_L^3}{V_\infty^3}\right)}$$

and the theoretical constant of proportionality is equal to 1.533 (Equation 6).

For any configuration sufficient data may be obtained to determine the variation of total drag for several values of the parameter (Equation 6) and subsequently determine the flight drag for the value of the parameter for flight conditions.

Figures (1) and (2) demonstrate the effectiveness of the correlation for two widely different configurations. It should be noted that the ASSET flight test data* are in good agreement with the estimated values based on this procedure.

* Not shown for security reasons.

CORRELATION OF VISCOUS AXIAL FORCE DATA

$12 < M < 21$

CONES AND MODIFIED CONES

$5° \leq \theta_c \leq 9°$

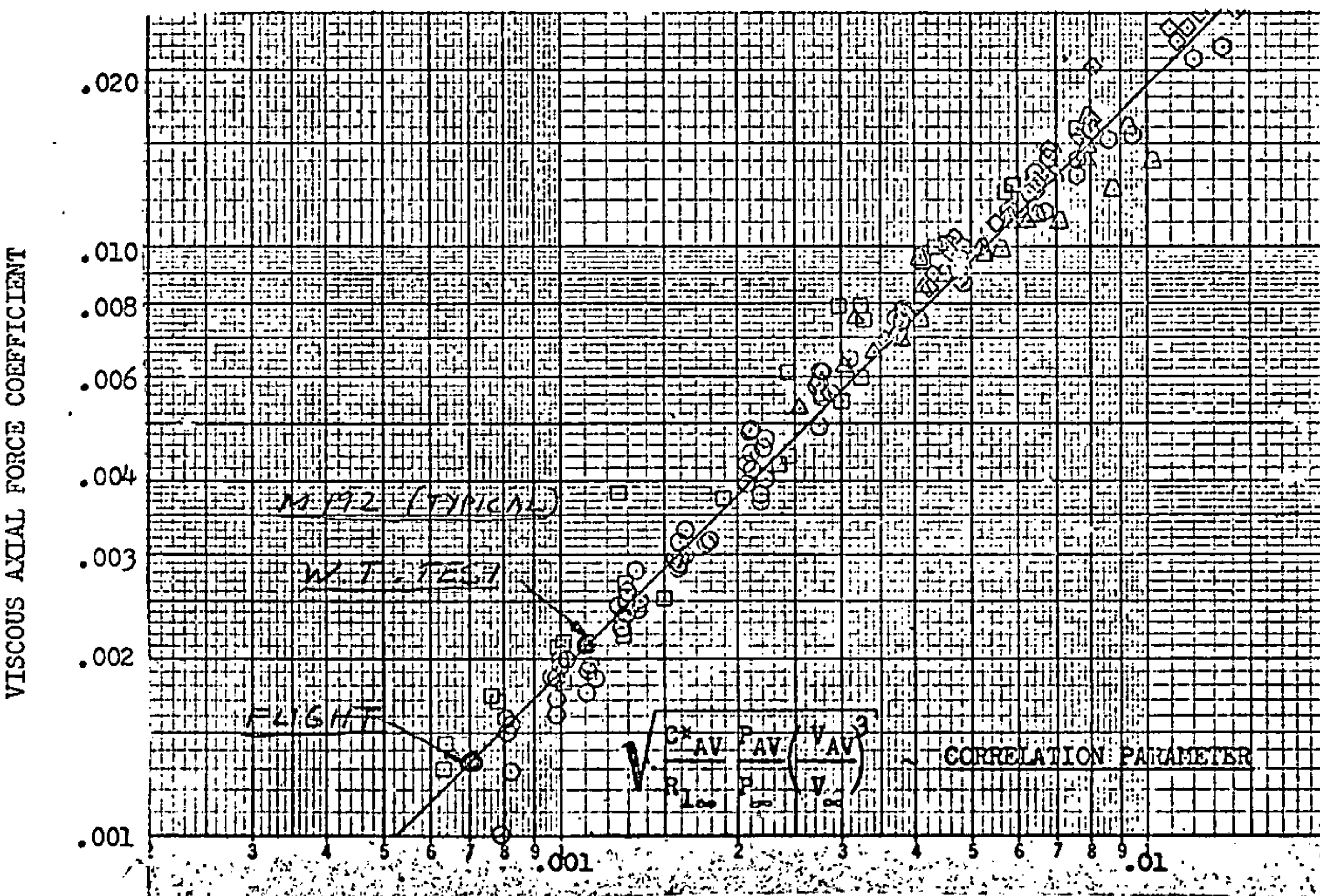

FIG. (1)

MCDONNELL

DATE ______ PAGE ______

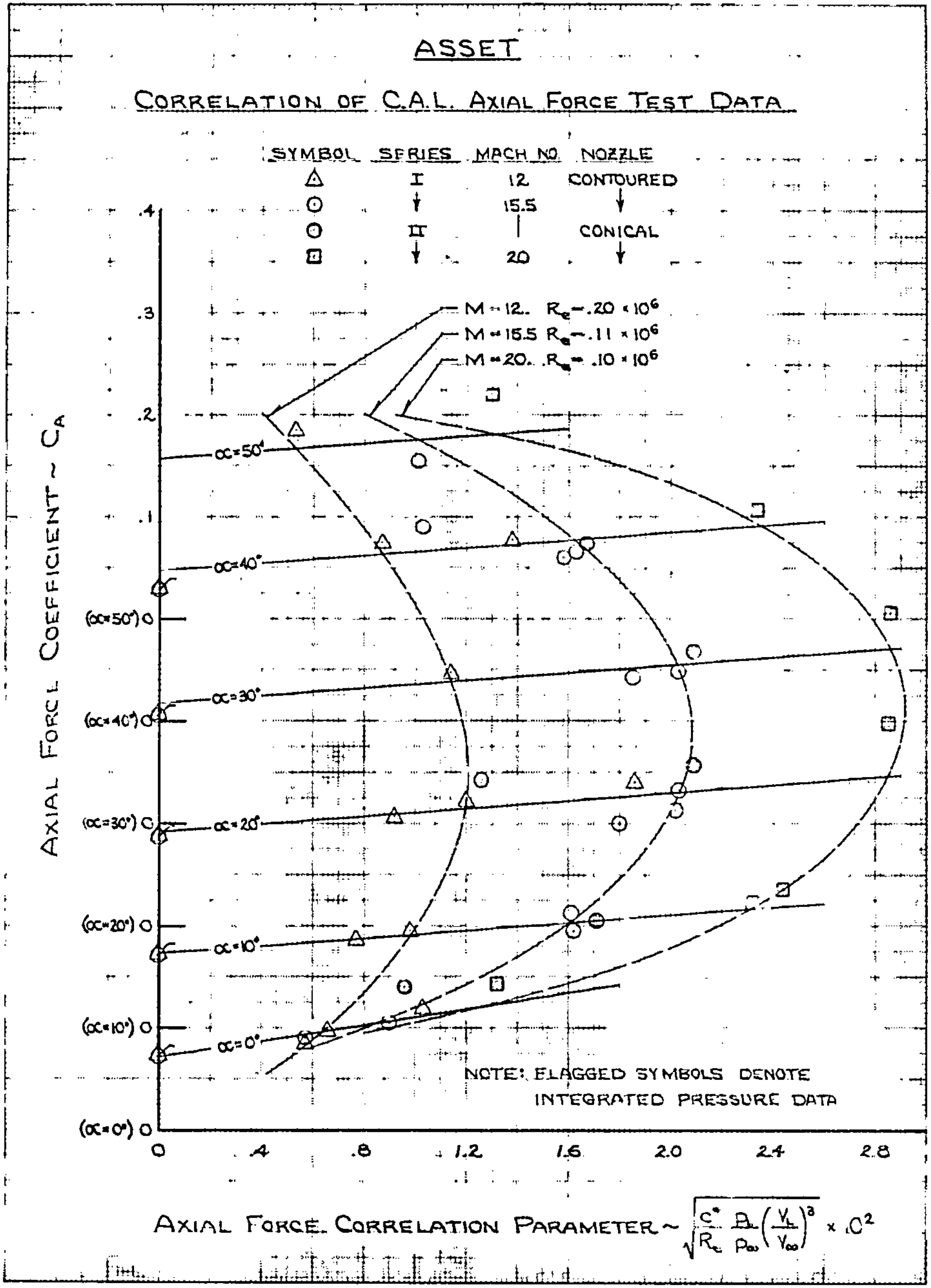

FIG. (2)

APPLICABLE McDONNELL EXPERIENCE

DESIGN-TEST-PRODUCTION

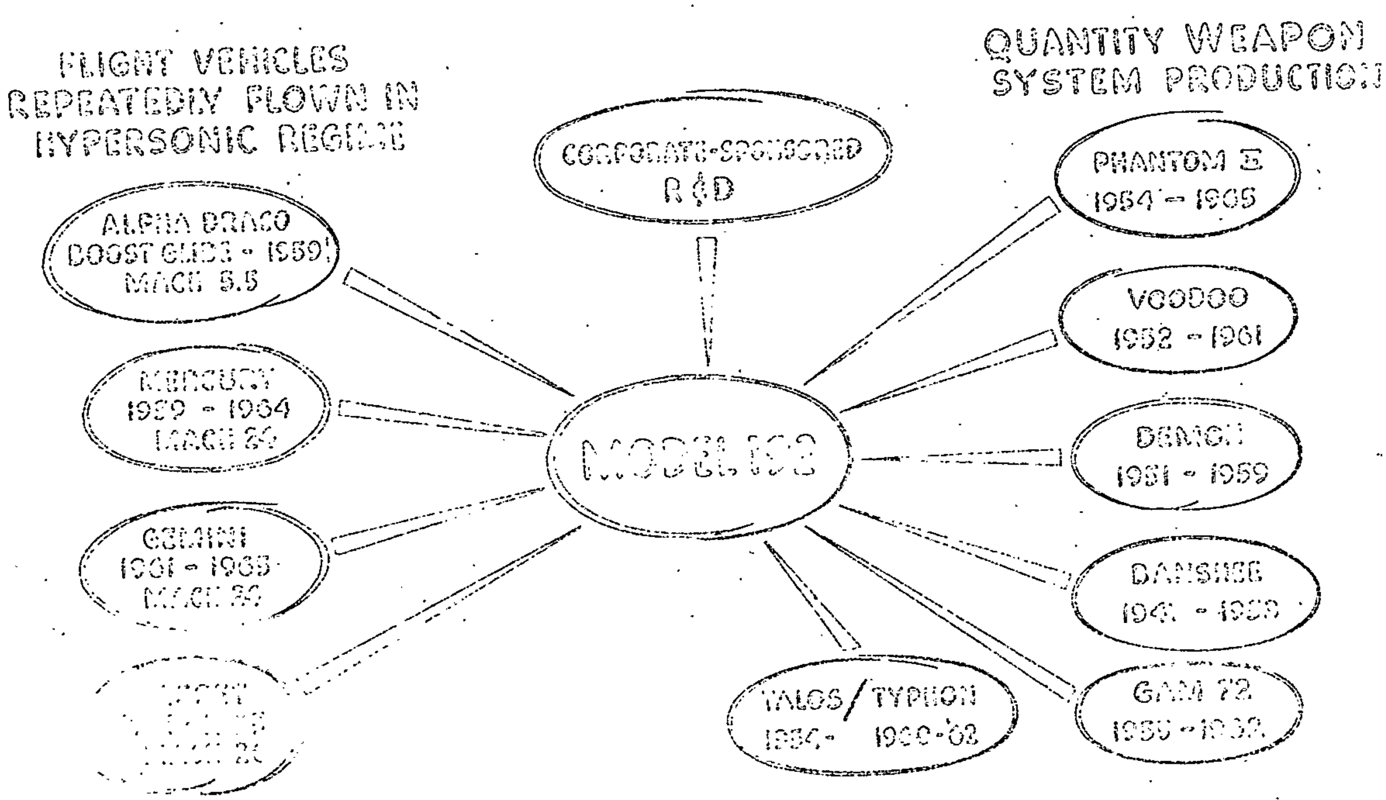

MAC SYSTEMS TIMETABLE

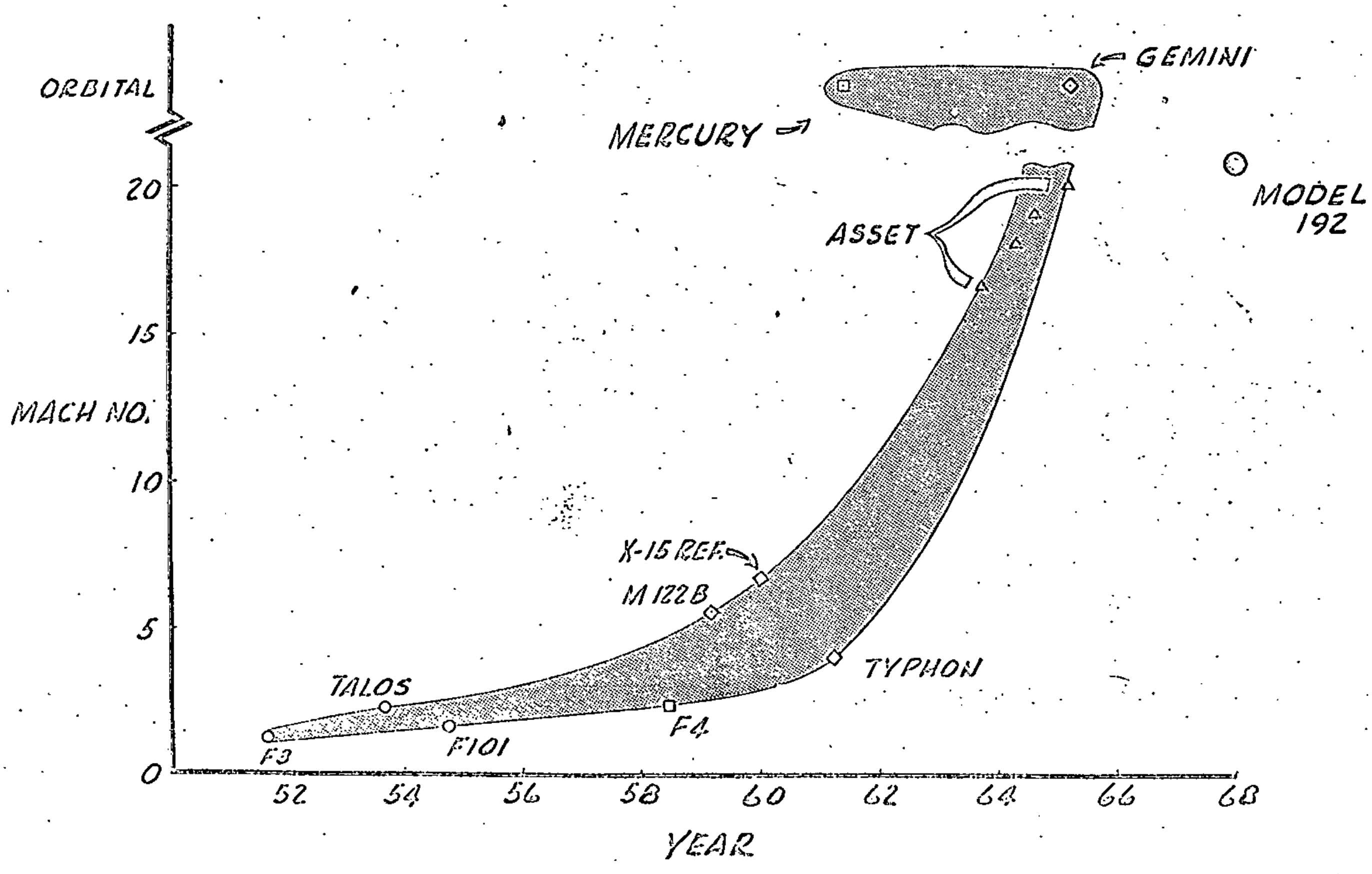

Declassified and Approved For Release 2013/11/21 : CIA-RDP71B00265R000200130005-0

HYPERSONIC PERFORMANCE

MACH 20

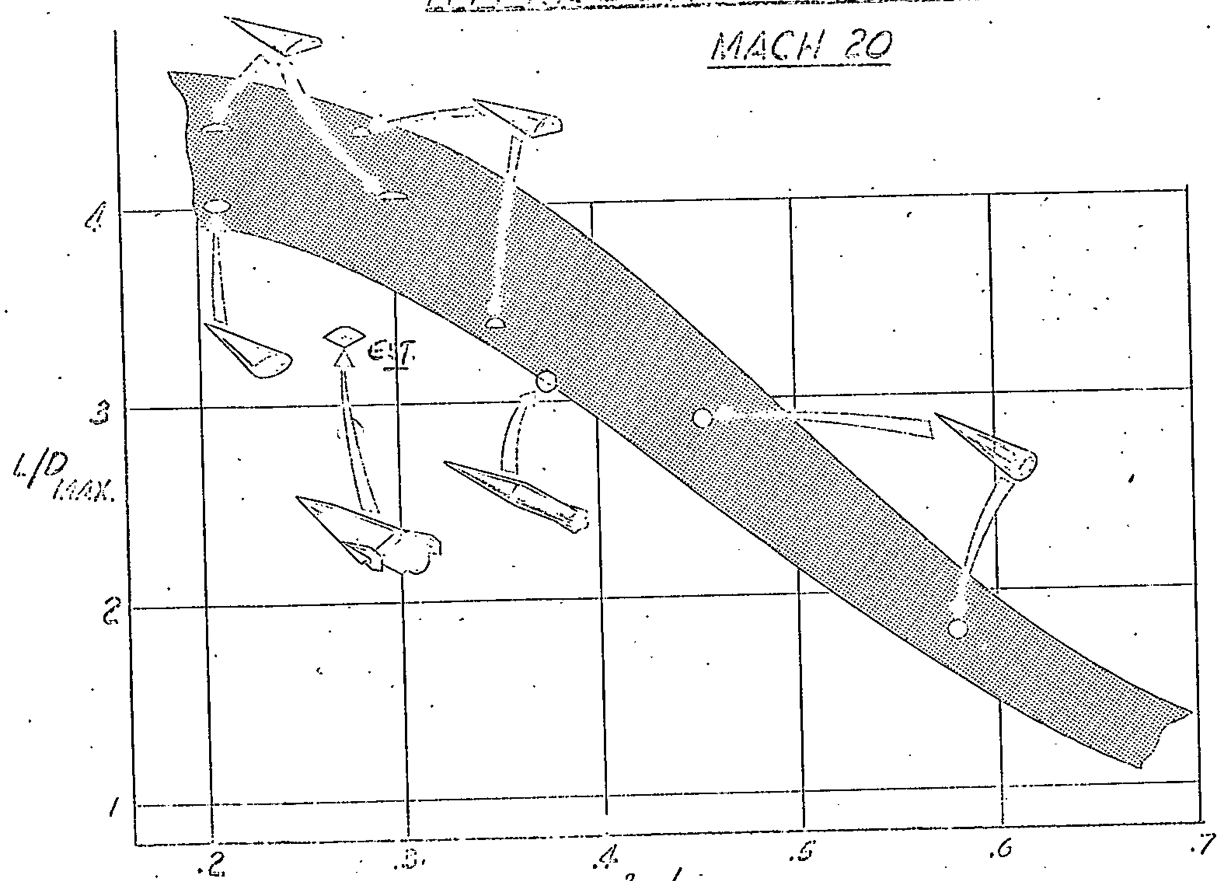

HYPERSONIC EFFICIENCY

M = 20

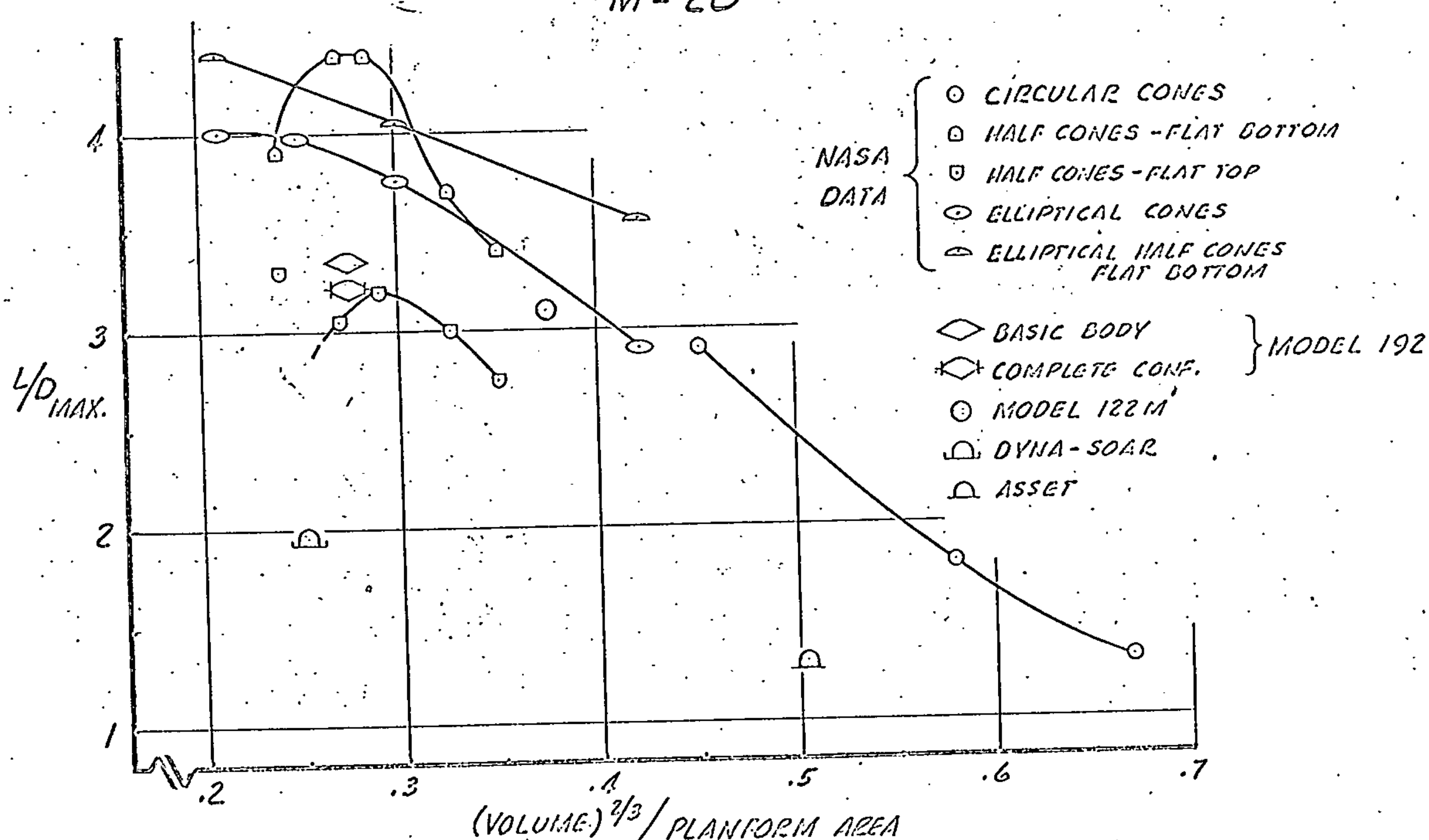

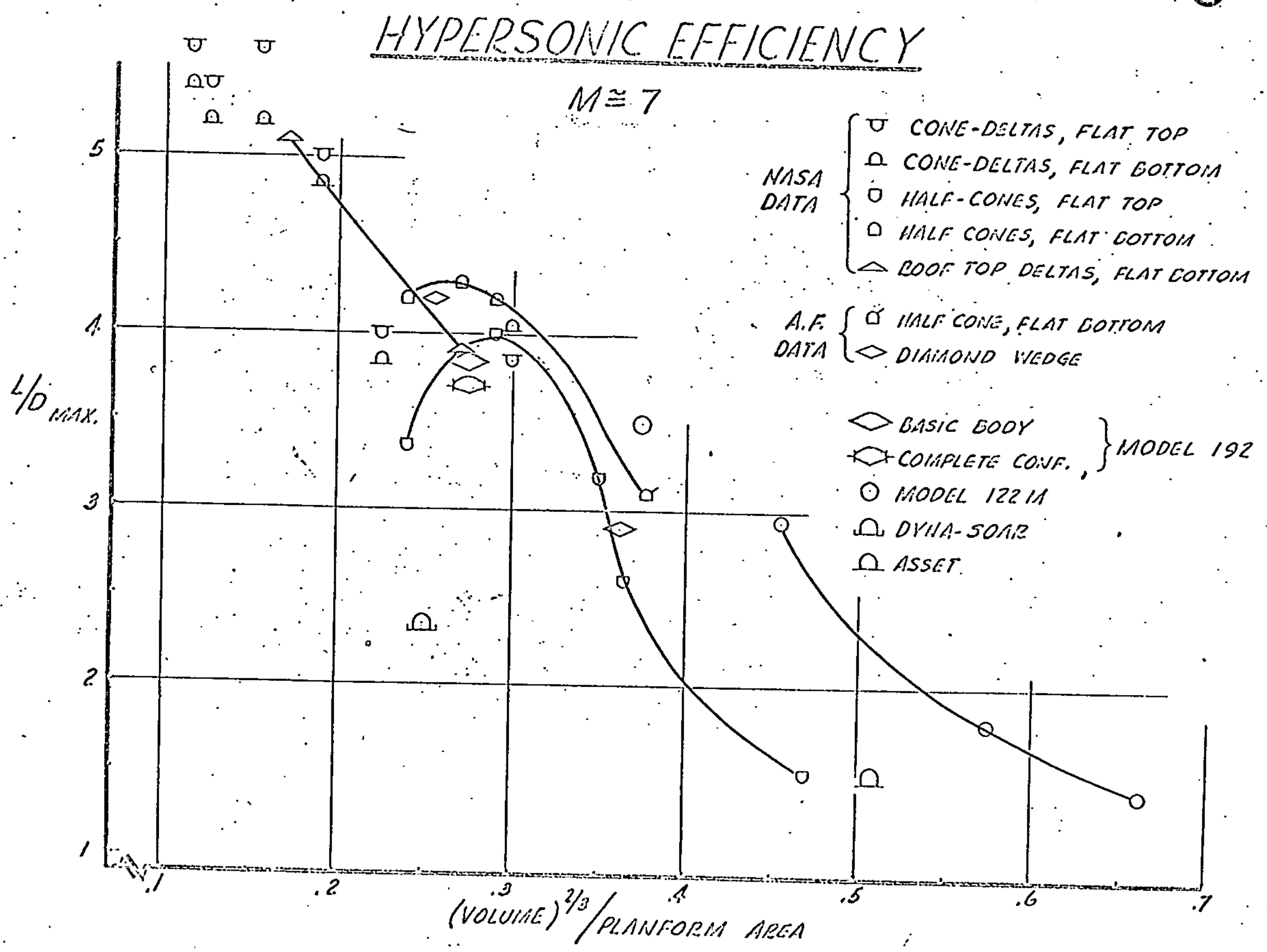
HYPERSONIC EFFICIENCY
M ≅ 7
NASA DATA
CONE-DELTAS, FLAT TOP
CONE-DELTAS, FLAT BOTTOM
HALF-CONES, FLAT TOP
HALF CONES, FLAT BOTTOM
ROOF TOP DELTAS, FLAT BOTTOM
A.F. DATA
HALF CONE, FLAT BOTTOM
DIAMOND WEDGE
BASIC BODY
COMPLETE CONF.
MODEL 192
MODEL 122 M
DYNA-SOAR
ASSET
L/D MAX.
5
4
3
2
1
.1
.2
.3
.4
.5
.6
.7
(VOLUME)^2/3/PLANFORM AREA

L/D SUBSTANTIATION

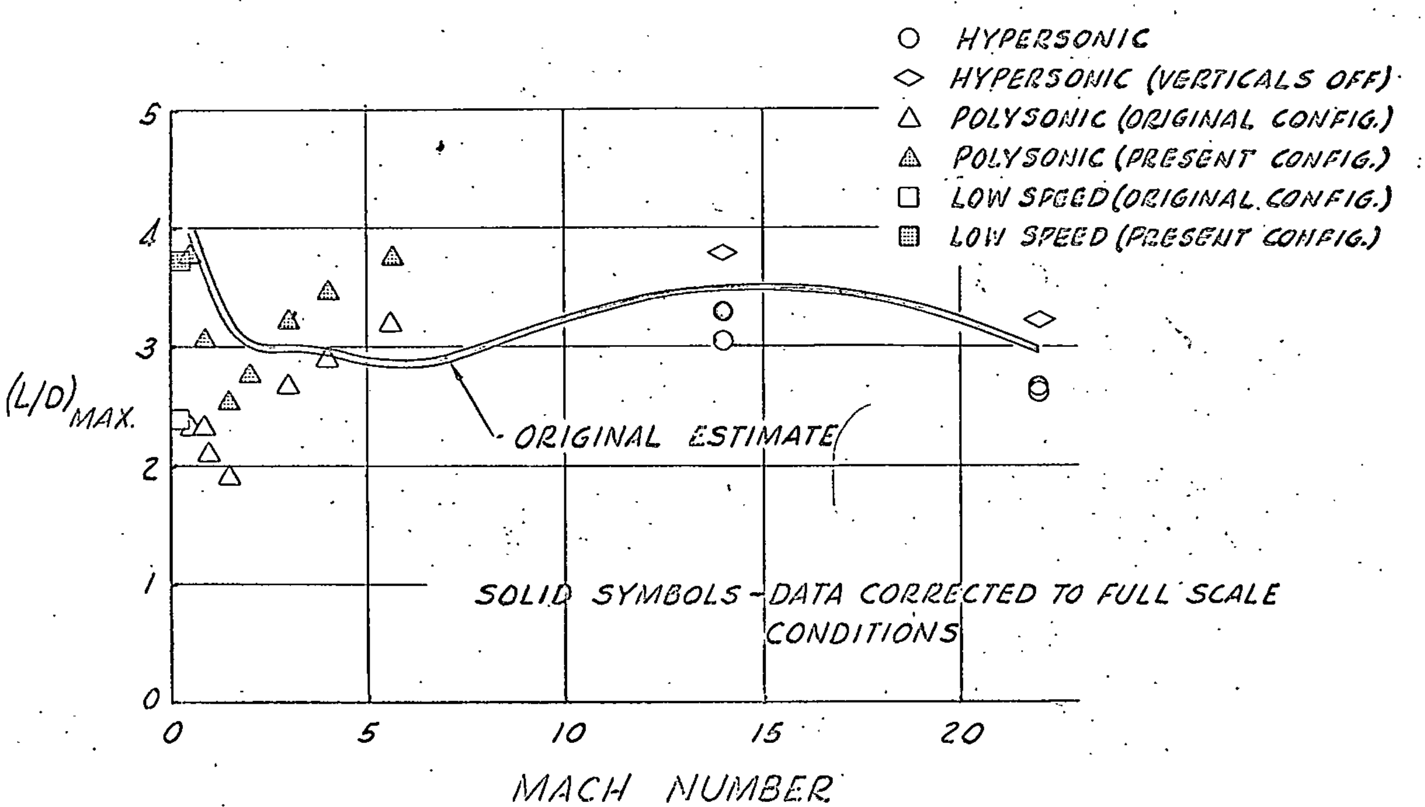

COATED COLUMBIUM PROPERTIES

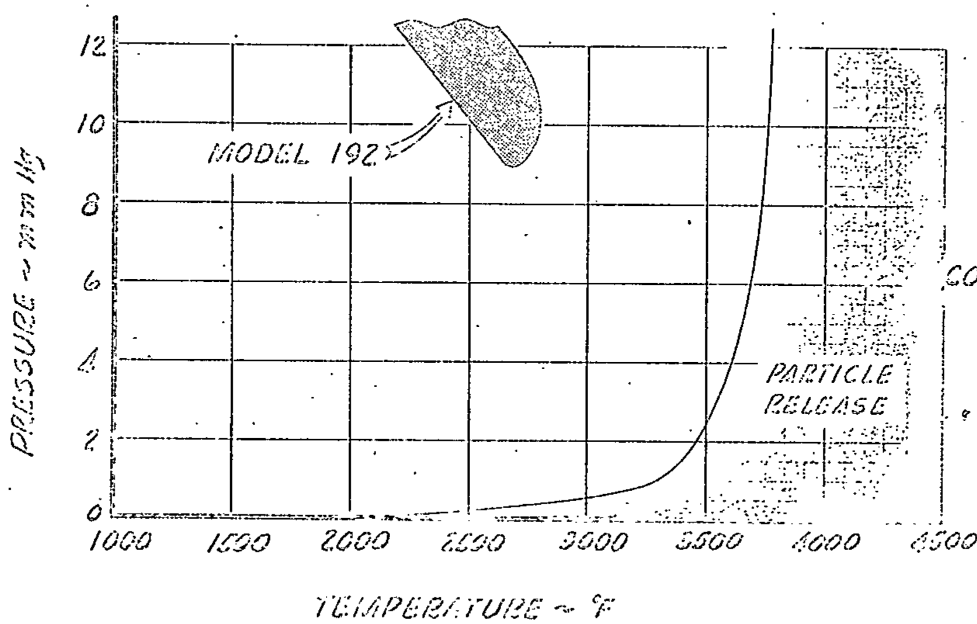

COMPOSITION

BASE MATERIAL	% WT.
CARBON	0.03 MAX.
HYDROGEN	0.0020 MAX.
OXYGEN	0.04 MAX.
NITROGEN	0.01 MAX.
ZIRCONIUM	2.0-3.0
TUNGSTEN	9.0-11.0
COLUMBIUM	85.9-89.0

COATING	
ALUMINUM	88
CHROMIUM	10
SILICONE	2

EJECTION CLEARANCE

TYPICAL ROCKET SEAT

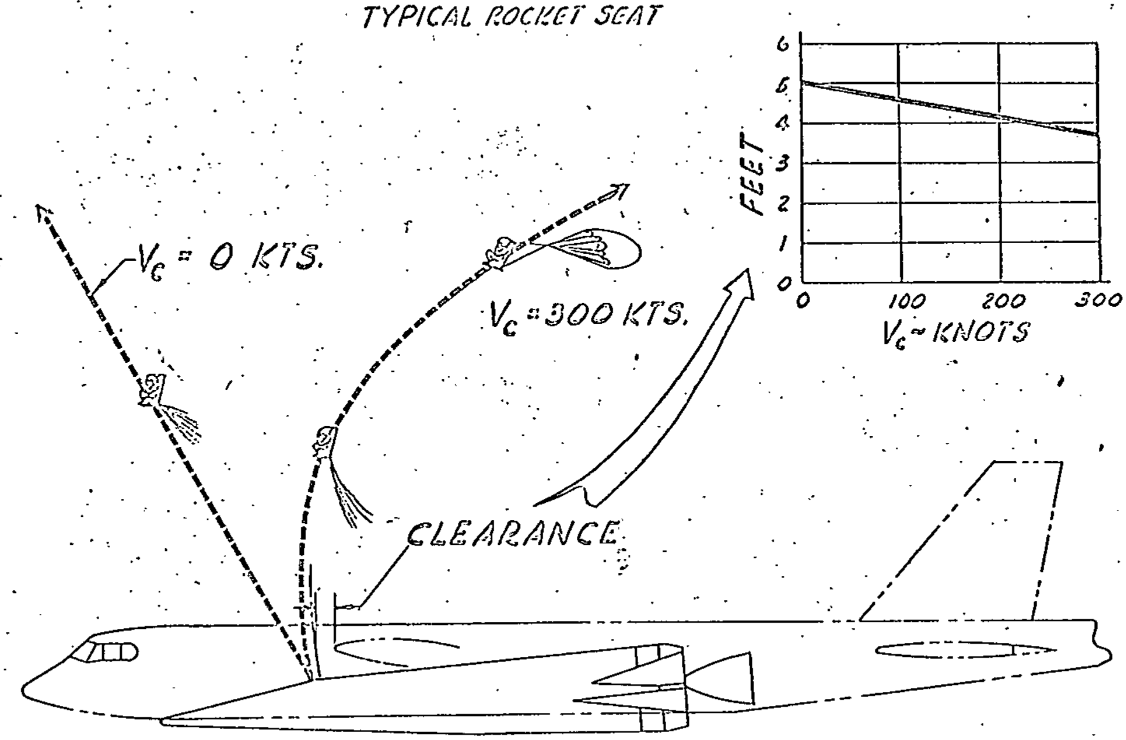

 PRELIMINARY

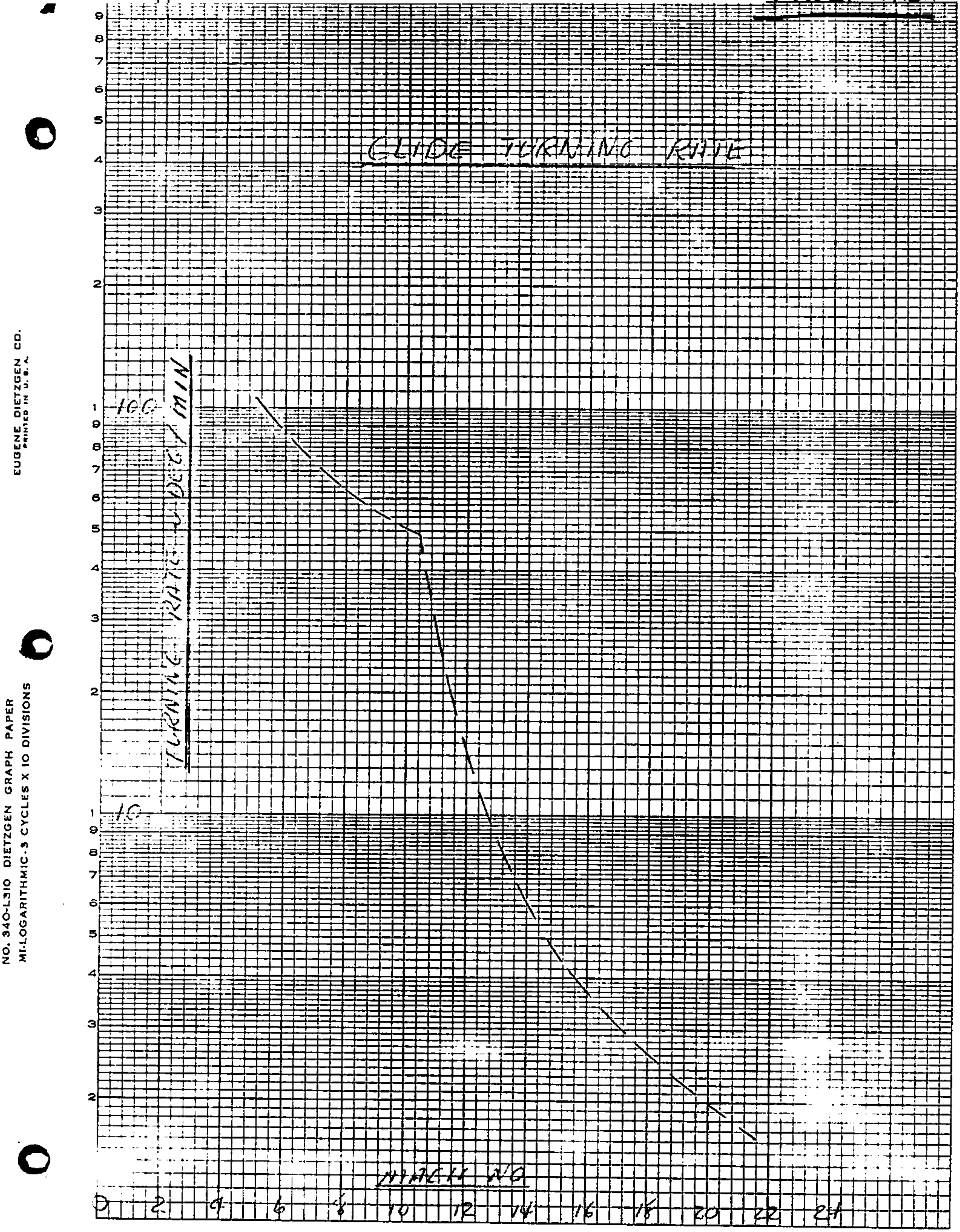

CENTRIFUGAL FORCE TERM

$$\dot{\gamma} = \frac{g_0}{V}\left\{ \frac{L+T\sin\delta_T}{W}\cos\phi - \left[\frac{R_0^2}{r^2} - \frac{V^2}{r} - \mu_3\frac{R_0^4}{r^4}\left(3\sin^2\lambda - 1\right)\right]\cos\gamma \right\}$$

OBLATENESS COEFFICIENT

CENTRIFUGAL FORCE DUE TO EARTHS ROTATION

$$\overbrace{+2\Omega\sin\psi\cos\lambda}^{\text{CORIOLUS ACCEL.}} + \frac{r\Omega^2}{V}\left[\cos^2\lambda\cos\gamma + \sin\gamma\cos\psi\sin\lambda\cos\lambda\right]$$

CORIOLUS TERM

$$\dot{\psi} = \frac{g_0}{V}\,\frac{L+T\sin\delta_T}{W}\,\frac{\sin\phi}{\cos\gamma} + 2\Omega\left[\sin\lambda - \tan\gamma\cos\lambda\cos\psi\right]$$

$$+\underbrace{\frac{V}{r}\sin\psi\cos\gamma\cos\lambda}_{\text{HEADING RATE ON A GREAT CIRCLE}} + r\Omega^2\,\frac{\sin\psi\sin\lambda\cos\lambda}{V\cos\gamma}$$

CENTRIFUGAL FORCE DUE TO EARTHS ROTATION

Let the earths rotation terms be zero, let $r = R_0 + h \sim R_0$, $\gamma \sim 0$, $T = 0$

then for $\dot{\gamma} = 0$ $\quad \frac{L}{W}\cos\phi = \left(1 - \frac{V^2}{gR_0}\right)$

if at the instant of concern $\psi = 0$ (Northerly heading)

$$\dot{\psi} = \frac{g_0}{V}\,\frac{L}{W}\sin\phi = \frac{g_0}{V}\,\frac{\left(1-\frac{V^2}{gR_0}\right)}{\cos\phi}\sin\phi = \frac{g_0}{V}\left(1 - \frac{V^2}{gR_0}\right)\tan\phi = \frac{g_0}{V}\left(1 - \left(\frac{V}{V_{SAT}}\right)^2\right)\tan$$

The limit bank angles correspond to an altitude such that

$$L/_W \cos\varphi = \left|1 - \frac{V^2}{gR_o}\right|$$

Thus

$$q = \frac{1 - V^2/_{gR_o}}{\cos\varphi} \; \frac{W}{C_L S}$$

Since φ is a function of MACH, and for a given velocity Mach is a function of altitude this equation must be solved by iteration. The results are shown here

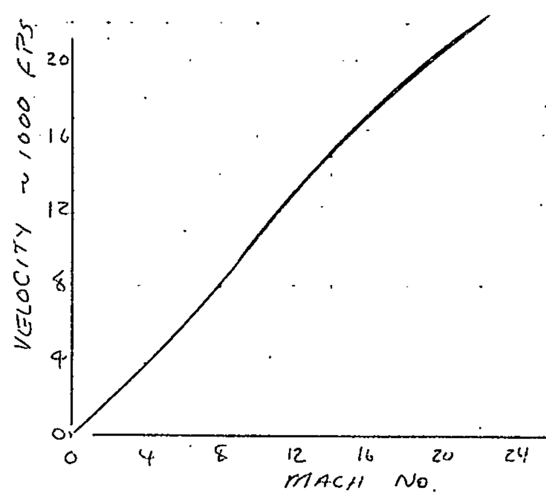

MACH	VELOCITY
21.5	21 300
16.0	19150
12.8	14100
10.4	10700
5.0	4850

Using this curve and the attached limit bank angle studies, the turn radius can be calculated.

PRELIMINARY

MANEUVERING CAPABILITY

GLIDE WEIGHT